Open Archive Toulouse Archive Ouverte

OATAO is an open access repository that collects the work of Toulouse researchers and makes it freely available over the web where possible

This is an author's version published in: http://oatao.univ-toulouse.fr/26901

Official URL:

https://doi.org/10.1109/CDC40024.2019.9030232

To cite this version:

Rakotondrabe, Micky and Al Janaideh, Mohammad *An RST control design based on interval technique for piezomicropositoning systems with rate-dependent hysteresis nonlinearities.* (2019) In: 2019 IEEE 58th Conference on Decision and Control (CDC), December 2019 (Nice, France).

Any correspondence concerning this service should be sent to the repository administrator: tech-oatao@listes-diff.inp-toulouse.fr

An RST Control Design Based on Interval Technique for Piezomicropositoning Systems with Rate-Dependent Hysteresis Nonlinearities

Micky Rakotondrabe[1] and Mohammad Al Janaideh[2]

***Abstract*— We propose a feedforward-feedback control of piezomicropositioing systems devoted to precise positioning over different operating conditions. Such systems exhibit rate-dependent hysteresis nonlinearities and badly damped oscillations characteristics. First, we introduce a rate-dependent Prandtl-Ishlinskii (RDPI) inverse model for feeforward compensation of hysteresis. This yields to compensation that can be characterized by an uncertain linear model with disturbances. To model the uncertainties, we suggest to use intervals then we propose a new interval design for a RST structured feedback controller. The proposed design method permits to satisfy prescribed performances. Simulation and experiments on a piezoelectric tube actuator are carried out and demonstrate the efficiency of the proposed control design.**

I. Introduction

Piezoelectric actuators are one of the most used actuators to develop precise positioning systems and to develop systems working at small scales. This recognition is thanks to the very interesting resolution (down to nanometer), the high bandwidth (up to tens of kHz), the high force density, and the low consumption they can offer [1]. In addition to that, piezoelectric actuators can be easily integrated as they are powered electrically. For instance, piezoelectric actuators are used in microrobotics for micromanipulation and microassembly applications [2] and in microscopes for fast images scanning [3].

Despite the above interesting properties of piezoelectric actuators, they are known to exhibit nonlinearities (hysteresis, creep) and badly damped oscillations in their responses. These compromise their overall performances during the positioning tasks and could even compromise the stability if in a closed-loop control scheme. Many studies have therefore been reported regarding the control and the attenuation of these phenomena, including feedforward scheme, feedback, and feedforward-feedback control schemes. Feedforward is particularly of great interest in applications where using sensors is not possible due to the lack of space. In counterpart, feedforward is very sensitive to modeling uncertainties and to external dirturbances. On the other hand, feedback and feedforward-feedback can offer robustness against model uncertainties additionally to specified performances satisfaction. Over feedback control, feedforward-feedback is able to furnish supplementary performances that feedback alone would not be able to give [4]. In this paper, we suggest the design of a feedforward-feedback control for piezoelectric actuators. The feedforward is to compensate for the rate-dependent hysteresis of the actuators and the additional feedback is to ensure performances robustness and to reject possible disturbances.

There are numerous studies regarding the modeling of hysteresis in piezoelectric actuators but few of them are extended to feedforward control. The latters include: the Bouc-Wen approach [5], the Preisach approach [6], and the Prandtl-Ishlinskii approach [7], [8], [9]. In the Prandtl-Ishlinskii approach, the rate-dependent Prandtl-Ishlinskii (RDPI) model is particularly able to approximate the hysteresis with shape changing versus the rate and versus the frequency of the driving input. In fact, much below the resonance frequency of many piezoelectric actuators, the hysteresis is observed to be yet rate-dependent. Taking into account such rate-dependency is essential in order to reduce modeling uncertainties and thus to increase the efficiency of a feedforward control scheme. This paper introduces first a RDPI model and its inverse to compensate for rate-dependent hysteresis in piezoelectric actuators. The compensation yields a linear model augmented with a bounded error that we will consider as an input disturbance. Then, the feedforward scheme is augmented with a feedback controller in order to ensure robustly certain prescribed performances. To that aim, a new design of the RST controller on the basis of interval techniques is proposed. The proposed RST controller is able to ensure *a priori* specified performances despite uncertain parameters in the linear model which we bound with interval numbers and despite input disturbance.

Interval techniques received many attention in states and parameters estimation [10], in robotics control [11] and in robustness analysis [12]. Regarding feedback controllers for interval systems, various techniques have been studied: interval PID structure [13], interval state-feedback structure [14], interval H_∞ technique [15], or interval controller based on performances inclusion design [16]. An advantage of writing uncertain parameters with interval numbers is the modeling simplicity. The controllers design itself is generally a combination of the

[1] Laboratoire Génie de Production, ENIT / Toulouse INP, Tarbes France, mrakoton@enit.fr

[2] Memorial University, St. John's, NL, Canada, maljanaideh@mun.ca

classical control tools with interval techniques. Relative to the above cited interval controllers design and the interval RST in [17], we propose a new RST controller that does not require solving inversion problem, which is therefore simpler.

II. RDPI FEEDFORWARD CONTROLLER

First the rate-dependent Prandtl-Ishlinskii (RDPI) model is reminded in this section. Then, the inverse of the model is given. Such inverse model is generally employed as feedforward controller, or compensator, for an actuator that exhibits a rate-dependent hysteresis. Finally, the error of compensation is reminded when the RDPI inverse model is not the exact inverse.

A. The model

Let $0 = t_0 < t_1 < \cdots < t_m$ be a partition of the interval $[0, T]$ such that v_r is monotone (nondecreasing or nonincreasing) in each interval $[t_{i-1}, t_i]$, $i = 1, \ldots, m$. A RDPI hysteresis model $\hat{\Phi}$ that approximates a real hysteresis Φ with input $v_r(t)$ and output $v(t)$ is defined as a superposition of n_h weighted rate-dependent play operators such that [7]

$$v(t) = \hat{\Phi}[u](t) = c_0 v_r(t) + \sum_{j=1}^{n_h} c_j \psi_{z_j(t)} \Delta(z_j(t)), \qquad (1)$$

where c_0 and c_j are the weights, $z_j(t) = \alpha j + \beta|\dot{v}_r(t)|$, $\psi_{z_j(t)}[v_r](t)$ is the rate-dependent play operator, and $\Delta(z_j(t))$ represents the distance between the dynamic thresholds. In this model, we have $\Delta(z_j(t)) = \alpha$. Each play operator $\psi_{z_j(t)}$, with $j = 1, \cdots, n_h$, is characterized by a dynamic threshold $z_j(t)$ and is described for $t \in]t_i, t_{i-1}]$ with $\eta_j(t) = \psi_{z_j(t)}$ as

$$\eta_j(t) = \max\{v_r(t) - z_j(t), \min\{v_r(t) + z_j(t), \eta(t_{i-1})\}\}, \qquad (2)$$

where $z_j(\dot{u}(t)) = \alpha j + \beta|\dot{u}(t)|$, where α and β are positive constant, and $v(0) = \max\{u(0) - r_j(0), \min\{u(0) + r_j(0), 0\}\}$. The fact that the play operator $\psi_{r_j(\dot{u}(t))}$ that composes the model $\hat{\Phi}$ have dynamic thresholds makes this latter rate-dependent. The identification of the RDPI model parameters is obatined using the shape function of the measured hysteresis loops [7].

B. The inverse model

The inverse of the RDPI model $\hat{\Phi}$ is denoted $\hat{\Phi}^{-1}$ and is called RDPI inverse model in the sequel. Its input is $v_r(t)$ and the output is $u(t)$. The RDPI inverse model $\hat{\Phi}^{-1}$ and the RDPI model $\hat{\Phi}$ have the same structure and are geometrically symmetrical. The shape function of inverse RDPI model is $\hat{\Phi}^{-1}$. Hence, the output of the inverse RDPI model $u(t) = \hat{\Phi}^{-1}$can be expressed as

$$u(t) = g_0 v_r(t) + \sum_{j=1}^{n_h} g_j \psi_{s_j(t)}[v_r](t) \Delta s_j(t), \qquad (3)$$

where $s_j(\dot{v}_r(t))$ are positive thresholds and g_0 and g_j are the weights of the inverse model. The dynamic threshold s_j and the weights g_0 and g_j are derived from the dynamic thresholds r_j and the weights c_0 and c_j [7].

C. The output of the Inverse Compensation and the error bounds

In this section we present an analytical formula for the output of the inverse compensation. Due to inexact inversion, the weights of the inverse model can be obtained as $j = i, \cdots, n_h$,

$$\Big(\sum_{j=0}^{i} c_i\Big)\Big(\sum_{j=0}^{i} g_i\Big) = 1 + \epsilon_j, \qquad (4)$$

$$\Delta z_j(t) = \Big(\sum_{j=0}^{i} c_i\Big)\Delta r_j(t) \qquad (5)$$

where $\epsilon_j \in \mathcal{R}$ is a constant representing uncertainties in the inverse RDPI model. We obtain the exact inversion when $\epsilon_j = 0$. Then, the output of the inverse compensation can be expressed as

$$v(t) = \delta_0 v_r(t) + \sum_{j=1}^{n_h} \delta_j \psi_{z_j(t)}[v_r](t) \Delta z_j(t), \qquad (6)$$

where $\Delta z_j(t) = \alpha$, $\delta_0 = 1 + \frac{\epsilon_0}{c_0}$, and $\epsilon \in \mathcal{R}$, and $|\epsilon| << 1$, and $\delta_j \in \mathcal{R}$ and $|\delta_j| << 1$. Then, we can write

$$v(t) = (1 + \epsilon_0) v_r(t) + \sum_{j=1}^{n_h} \epsilon_j \psi_{z_j(t)}[v_r](t), \qquad (7)$$

where $\epsilon_j = \delta_j \alpha$. For exact compensation, $\epsilon_0 = 1$ and $\epsilon_j = 0$. Then, $v(t) = v_r(t)$. The output of the inverse compensation is

$$v(t) = v_r(t) + \epsilon v_r(t) + \sum_{j=1}^{n_h} \epsilon_j \big(v_r(t) - \Gamma_{z_j(t)}\big)[v_r](t), \qquad (8)$$

where $\Gamma_{z_j(t)}$ is the output of the rate-dependent stop operator, with $\Gamma_{z_j(t)}[v_r](t) = v_r(t) - \Psi_{z_j(t)}[v_r](t)$. Let $\gamma_j(t) = \Gamma_{z_j(t)}$, then for $t \in]t_{i+1}, t_i]$

$$\gamma_j(t) = \min\{z_j(t), \max\{-z_j(t), v_r(t) - v_r(t_i) + \gamma_j(t_i)\}\}. \qquad (9)$$

and the output of the inverse compensation can be expressed as

$$v(t) = v_r(t)\left(1 + \sum_{j=0}^{n_h} \epsilon_j\right) - \sum_{j=1}^{n_h} \epsilon_j \Gamma_{z_j(t)}[v_r](t). \qquad (10)$$

The error of the inverse compensation can be presented as $e(t) = v_r(t) - v(t)$, then

$$e(t) = -v_r(t) \sum_{j=0}^{n_h} \epsilon_j + \sum_{j=1}^{n_h} \epsilon_j \Gamma_{z_j(t)}[v_r](t). \qquad (11)$$

We can conclude that $|\Gamma_{z_j(t)}[v_r](t)| \leq z_j(t)$, then

$$|e(t)| \leq |v_r(t)| \sum_{j=0}^{n_h} |\epsilon_j| + \sum_{j=1}^{n_h} |\epsilon_j||z_j(t)|. \qquad (12)$$

Since $z_j(t) = \alpha j + \beta|\dot{v}_r(t)|$

$$|e(t)| \leq |v_r(t)|\sum_{j=0}^{n_h}|\epsilon_j| + \alpha\sum_{j=1}^{n_h}|\epsilon_j|j + \beta\sum_{j=1}^{n_h}|\epsilon_j||\dot{v}_r(t)|. \quad (13)$$

Let $\delta_0 = |\epsilon_0|$ and $\delta = \max|\epsilon_j|$, where $j = 1, \cdots, n_h$. Then we conclude that the error bounds is

$$|e(t)| \leq \underbrace{|v_r(t)|\delta_0 n_h + \alpha n_h \delta}_{\text{Rate-Independent}} + \underbrace{\beta n_h \delta|\dot{v}_r(t)|}_{\text{Rate-Dependent}} \quad (14)$$

Then we can write

$$v(t) = v_r(t) + b(t), \quad (15)$$

where $b(t)$ is the error of the compensation.

D. The new model

Eq. (15) provides a linear relation between the new input $v_r(s)$ and the output displacement $y(s)$ of the piezoelectric actuator. This relation is valid at frequencies lower than the resonance where the RDPI model is identified. To extend the model in order to account for the dynamics of the actuator, the Hammerstein structure is suggested. It consists in considering the actuator behavior as a cascade of a nonlinear part valid at low frequency and a linear dynamics. Hence Fig. (1-a) represents the Hammerstein scheme augmented with the RDPI inverse model. The actuator is represented here with the RDPI hysteresis model and a normalized linear dynamics $D(s)$, with $D(s = 0) = 1$. Considering Eq. (15), a new linear dynamical model $G(s) = kD(s)$ is therefore obtained as schemated in Fig. (1-b) where the input disturbance is: $d(s) = b(s)D(s)$.

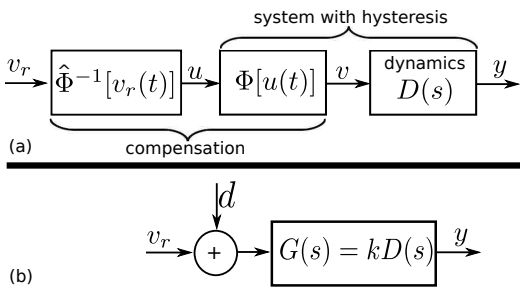

Fig. 1: (a): the compensation scheme. (b): the new system.

In most of applications of piezoelectric actuators, a 2nd order model is sufficient. Indeed, it accounts for the bandwidth and for the first resonance while the model remains simple. Therefore, we consider the following 2nd order model:

$$G(s) = k.D(s) = \frac{k}{\frac{1}{\omega_n^2}s^2 + \frac{2\zeta}{\omega_n}s + 1} \quad (16)$$

where ω_n is the natural frequency and ζ is the damping coefficient.

Due to the high sensitivity of miniaturized systems face to the environment however, their model parameters are uncertain [18]. Piezoelectric actuators are specifically very sensitive to temperature variation and to surrounding vibration. Whilst developing a temperature-dependent model of piezoelectric actuators might become a very tricky task due to the lack of studies regarding the precise effects of thermal variation, it is however of great interest to be able to at least consider and model these effects as uncertainties. One way in the litearature to model in an easy way such uncertainties in piezoelectric actuators models is intervals [14], [16]. Once an interval model is obtained, interval techniques can be combined with control techniques to synthesize a robust controller that will further ensure the stability and the performances of the closed-loop despite the uncertainties ranging in the intervals. Because of this easy way to bound uncertainties, we suggest to use interval models in this paper. Thus, "point" model in Eq. (16) becomes:

$$[G](s) = \frac{[k]}{\frac{1}{[\omega_n]^2}s^2 + \frac{2[\zeta]}{[\omega_n]}s + 1} = \frac{[k]}{[a_2]s^2 + [a_1]s + 1} \quad (17)$$

such that the static gain, the natural frequeny and the damping ratio of the actuator model are uncertain but within the intervals $[k]$, $[\omega_n]$ and $[\zeta]$, respectively.

III. An interval RST feedback controller design

Having the interval model in Eq. (17) to approximate the behavior of the piezoelectric actuator with the RDPI inverse model (hysteresis compensator), we propose to add a feedback controller in order to reject any disturbance, including the internal disturbance $d(s)$ due to compensation error, and to satisfy certain prescribed tracking performances. We propose here a RST controller feedback structure as it is known to be robust against disturbance additionally to its robustness to ensure static error deletion.

A. Structure

Let Fig. (2-a) (equivalently Fig. (2-b)) represent the new model augmented with a RST structured feedback controller. Despite the fact that RST controllers were originally and were systematically designed in the discrete-domain, we propose here a continous-domain design combined with interval models. Therefore, R, S and T are polynomials in the Laplace variable s.

In the classical version, i.e. without using intervals, the basic idea of the RST controller is to find the polynomials R, S and T such that the feedback in Fig. (2-a) has its poles equal to imposed/specified poles. This is why the RST approach is among the poles assignment approaches. The found controller will even reject an input disturbance d if certain conditions are satisfied during

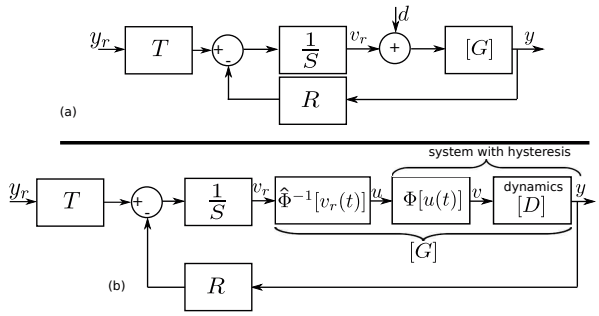

Fig. 2: (a): the RST controller applied to the new system. (b): details with the RDPI inverse model.

the design steps. Since we are dealing with intervals, we propose an interval RST controller design. In this case, the specifications are also intervals. One important result in interval techniques that will be used during the further design is the performances inclusion in interval transfer functions. This is reminded in Section- (III-B).

B. Performances inclusion for stable transfer functions

Performances inclusion in interval transfer functions has been used for controllers synthesis [16] and for actuators structures design [2]. We will use this to further design the RST feedback controller. The theorem contains two properties: one property for the frequency domain performances and one property for the time domain performances.

Consider two stable interval systems having the same polynomials degrees m and n:

$$[H_1](s) = \frac{\sum_{l=0}^{m} [p_{1l}] \cdot s^l}{\sum_{k=0}^{n} [q_{1k}] \cdot s^k} \quad , \quad [H_2](s) = \frac{\sum_{l=0}^{m} [p_{2l}] \cdot s^l}{\sum_{k=0}^{n} [q_{2k}] \cdot s^k} \tag{18}$$

Theorem 3.1: Performances inclusion theorem [12].

In the frequency domain:

$$if \begin{cases} [q_{1k}] \subseteq [q_{2k}], \quad \forall k = 1 \cdots n \\ and \\ [p_{1l}] \subseteq [p_{2l}], \quad \forall l = 1 \cdots m \end{cases} \Rightarrow \begin{cases} [\rho]([H_1](j\omega)) \subseteq [\rho]([H_2](j\omega)) \\ and \\ [\varphi]([H_1](j\omega)) \subseteq [\varphi]([H_2](j\omega)) \end{cases}$$

In the time domain:

$$if \begin{cases} [q_{1k}] \subseteq [q_{2k}], \quad \forall k = 1 \cdots n \\ and \\ [p_{1l}] \subseteq [p_{2l}], \quad \forall l = 1 \cdots m \end{cases} \Rightarrow \quad [h_1](t) \subseteq [h_2](t)$$

where $[\rho]([H_i](j\omega)$ is the set of magnitude of the interval system $[H_i]$, $[\varphi]([H_i](j\omega)$ is its argument and $[h_i](t)$ is the impulse response of the two systems.

As a definition, we say that $[H_1](s) \subseteq [H_2](s)$ when $[q_{1k}] \subseteq [q_{2k}]$ and $[p_{1l}] \subseteq [p_{2l}]$.

C. Problem formulation

Let us decompose $[G](s)$ as: $[G](s) = \frac{[B](s)}{[A](s)}$ with $[B](s) = [k]$ and $[A](s) = [a_2]s^2 + [a_1]s + 1$. From Fig. (2-a), we obtain

$$y(s) = \frac{[B]T}{([A]S + [B]R)} y_r(s) + \frac{[B]S}{([A]S + [B]R)} d(s). \tag{19}$$

Our target is to find the RST controller s.t. the controller reject the effect of the disturbance $d(s)$ and s.t. a desired tracking performance described by a desired closed-loop interval transfer function $[H_d](s)$ be satisfied. That is

- disturbance rejection: to ensure disturbance rejection, the transfer function that links $d(s)$ and $y(s)$ should contain at least one zero, i.e. $S(s)$ should be of the following structure:

$$S(s) = s^z S_z(s), \tag{20}$$

where $S_z(s)$ is a polynomial with a relative degree of z with regards to $S(s)$.

- tracking performance: according to the performances inclusion result in Theorem- (III-B), the following inclusion permits to the closed-loop to satisfy the desired specification described by $[H_d](s)$:

$$\frac{[B](s)T(s)}{([A](s)S(s) + [B](s)R(s))} \subseteq [H_d](s) \tag{21}$$

Indeed, Eq. (21) satisfies $y(s) \subseteq [H_d](s) y_r(s)$ and thus the output follows prescribed and desired evolution.

D. Rewriting the problem

Let us decompose the desired closed-loop transfer function as: $[H_d](s) = \frac{[B_m](s)}{[A_m](s)}$ where $[A_m](s)$ will be called interval reference polynomial. For existence of solution, $deg[A_m] \geq 2 \times deg[A]$. In the sequel we take: $deg[A_m] = 2 \times deg[A]$. Therefore, the above RST controller design problem becomes in finding the polynomials $R(s)$, $S(s)$ and $T(s)$ such that we satisfy the following conditions:

- condition-1: for disturbance rejection, let us consider that $S(s)$ exhibits one zero, i.e. $z = 1$. This is because we do not know the order of S at this time and because we will have more degrees of freedom in S by minimizing z. In counterpart, only low frequency disturbance will be rejected when the relative degree z is low. Because the disturbance d is due to error of hysteresis compensation that is supposed to be much below the resonance frequency, $z = 1$ is sufficient, i.e.:

$$S(s) = s.S_1(s) \tag{22}$$

- condition-2: from Inclusion. (21), we have:

$$[A](s)S(s) + [B](s)R(s) \subseteq [A_m](s) \tag{23}$$

Inclusion. (23) is an interval inclusion version of the Diophantine equation.

- condition-3: from Inclusion. (21), we also have:

$$[B](s)T(s) \subseteq [B_m](s) \tag{24}$$

- condition-4: finally, similarly to Diophantine equation [19], the Diophantine inclusion in Inclusion. (23) has unique solutions iff:

$$deg(R) = deg([A]) \tag{25}$$

This unicity of solutions is to ensure that one has the same number of independent inclusions and of unknown variables.

Considering condition-1 ($S(s) = s.S_1(s)$) and the closed-loop transfer function $\frac{[B](s)T(s)}{([A](s)S(s)+[B](s)R(s))}$ however, the RST controller ensures a zero steady-state tracking performance error by taking:

$$T(s=0) = R(s=0) \tag{26}$$

Hence, the problem finally becomes:

Problem 3.1: Find the polynomials $R(s)$, $S(s)$ and $T(s)$ s.t.:

a) Robust disturbance rejection:

$$S(s) = s.S_1(s)$$

b) Tacking performances through Diophantine inclusion:

$$[A](s)S(s) + [B](s)R(s) \subseteq [A_m](s)$$

c) Numerator inclusion to complete the tracking performances:

$$[B](s)T(s) \subseteq [B_m](s)$$

d) Robust steady-state tracking performance:

$$T(s=0) = R(s=0)$$

e) Unicity of solution for the Diophantine inclusion:

$$deg(R) = deg([A])$$

Note that the disturbance rejection and the steady-state tracking performances are said robust here because they will be ensured independently to the model parameters. On the other hand, the transient part tracking performances are also said robust because, through the Diophante inclusion, the controller will ensure the specifications for any uncertainties of the model parameters described by intervals $[A](s)$ and $[B](s)$.

Because $[B](s) = [k]$ and because of condition-d of Problem. (3.1), we can keep $T(s)$ as a static gain for the sake of simplicity: $T(s) = R(s=0)$. Hence, $[B_m]$ is a static gain according to condition-c of Problem. (3.1). In this case, condition-c is not used to calculate any controller parameters since $R(s=0)$, and thus $T(s) = R(s=0)$ is already calculated from the Diophantine inclusion in condition-b. $[B_m]$ can be taken to be: $[B_m] = [k]R(s=0)$, which also satisfies condition-c and is thus defined *a posteriori* , i.e. once $R(s=0)$ is calculated.

E. Choice of the desired interval transfer function

The suggested RST interval controller design requires a desired interval transfer function $[H_d](s)$. This reference interval transfer function is a transcription of the desired and specified tracking performances for the closed-loop. Let us take the following tracking performances specifications:

- the settling time t_r of the closed-loop should be less or equal to t_{rmax}. Thus an interval desired settling time can be created as follows: $[t_r] = [0, t_{rmax}]$,

- no oscillation is desired in the step-response of the closed-loop.

A first order system of type $\frac{1}{(\frac{[t_r]}{3}s+1)}$ can be a transcription of the above specifications. Taking into account the fact that $deg[A_m] = 2 \times deg[A] = 4$, the following structure is given for $[H_d](s)$:

$$[H_d](s) = \frac{[k]R(s=0)}{\left(\frac{[t_r]}{3}s+1\right)\left(\frac{[t_r]}{3n_f}s+1\right)^3} = \frac{[B_m](s)}{[A_m](s)} \tag{27}$$

where $n_f > 1$ is an integer to maintain the first order part $\frac{1}{(\frac{[t_r]}{3}s+1)}$ dominant. For that we take $n_f = 30$.

F. Resolution

The resolution of the RST controller is an iteration solving of the 5 conditions in Problem. (3.1), except condition-c. The iteration process is presented below.

From conditon-e, we impose

$$R(s) = \rho_2 s^2 + \rho_1 s + \rho_0, \tag{28}$$

where ρ_2, ρ_1 and $\rho_0 = R(s=0)$ are parameters to be sought for.

Then, because $deg([A_m]) = 4$, from the Diophantine equation in condition-b, we should have $deg(S) = 2$. Hence, considering condition-a, we impose

$$S(s) = s(\mu_1 s + \mu_0), \tag{29}$$

where μ_1 and μ_0 are parameters to be sought for.

Introducing Equ. (28) and Equ. (29) in the Diophantine inclusion in condition-b, we have

$$\begin{aligned}&\mu_1[a_2]s^4 + (\mu_1[a_1] + \mu_0[a_2])\,s^3 + (\mu_1 + \mu_0[a_1] + [k]\rho_2)\,s^2 \\ &+ (\mu_0 + [k]\rho_1)\,s + [k]\rho_0 \subseteq \frac{[t_r]^4}{81n_f^3}s^4 + \frac{[t_r]^3}{9n_f^2}\left(1+\frac{1}{3n_f}\right)s^3 \\ &+ \frac{[t_r]^2}{3n_f}\left(1+\frac{1}{n_f}\right)s^2 + \frac{[t_r]}{3}\left(1+\frac{1}{n_f}\right)s + 1\end{aligned} \tag{30}$$

Finally, from Inclusion. (30) and from condition-d, the RST controller parameters are therefore calculated to

satisfy the following inclusions:

$$\begin{cases} \mu_1 \in \frac{[t_r]^4}{81 n_f^3 [a_2]} \\ \mu_0 \in \frac{1}{[a_2]} \left(\frac{[t_r]^3}{9 n_f^2} \left(1 + \frac{1}{3n_f}\right) - \mu_1 [a_1] \right) \\ \rho_2 \in \frac{1}{[k]} \left(\frac{[t_r]^2}{3 n_f} \left(1 + \frac{1}{n_f}\right) - \mu_1 - \mu_0 [a_1] \right) \\ \rho_1 \in \frac{1}{[k]} \left(\frac{[t_r]}{3} \left(1 + \frac{1}{3n_f}\right) - \mu_0 \right) \\ \rho_0 \in \frac{1}{[k]} \\ T(s) = \rho_0 \end{cases} \tag{31}$$

As from Inclusion. (31), the derivation of the controller avoids set inversion problem and thus is straightforward in calculation.

G. The controller

Once the parameters of $R(s)$, $S(s)$ and $T(s)$ calculated, the controller is implemented. The scheme in Fig. (2) is not implementable because $T(s)$ and $R(s)$ are not causal. Instead, the scheme in Fig. (3) is used where $\frac{T(s)}{R(s)}$ is strictly causal and $\frac{R(s)}{S(s)}$ is causal non-strictly:

$$\frac{T(s)}{R(s)} = \frac{\rho_0}{\rho_2 s^2 + \rho_1 s + \rho_0} \tag{32}$$

$$\frac{R(s)}{S(s)} = \frac{\rho_2 s^2 + \rho_1 s + \rho_0}{s(\mu_1 s + \mu_0)} \tag{33}$$

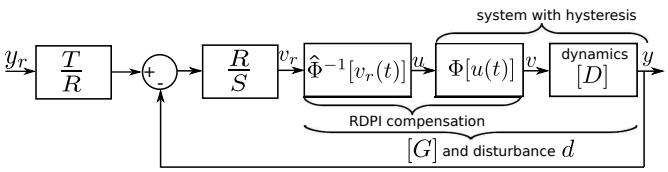

Fig. 3: Implementation of the RST controller and of the RDPI compensator.

IV. Experimental results

The application of the proposed interval RST controller design to a piezoelectric actuator is presented in this section.

A. The experimental setup

The piezoelectric actuator to be used has a tubular structure. Piezoelectric tube actuators are actually the original principal actuator in atomic force microscopy (AFM) [3] for images scanning applications. Nowadays, piezoelectric tube actuators can also be used for nanomanipulation applications [20]. The tube actuator has one internal electrode that serves as electrical ground and four external electrodes to which four independent electrical potentials can be applied. Accoding to the applied potentials, a bending of the tube along x-axis, a bending along y-axis and an expansion along z-axis (the tube axis) is obtained. In this paper, we only study the bending (displacement) along y-axis.

The used experimental setup includes the piezoelectric actuator referenced as PT 230.94 from the *PI* company and which has $30mm$ of length and $3.2mm$ of external diameter. The internal diameter is $2.2mm$. The actuator voltage in this study will be ranging up to $\pm 100V$. A displacement sensor that measures the y bending at the tip of the piezotube actuator. The sensor principle is inductive and is the reference ECL202 from *LionPrecision* company. A computer from which the driving voltage is generated, the controller is implemented and the measurement is acquired. Matlab-Simulink software is used for that. A dSPACE acquisition board, referenced as dS1104, serves as interface and contains the DAC (digital to analogic) and ADC (analogic to digital) converters. Since the voltage from the computer and the dSPACE acquisition board is limited to $\pm 10V$, a voltage amplifier with a gain of 20 is also used.

B. Characterization and hysteresis compensation

The hysteresis behavior of the piezoelectric actuator is displayed in Fig. (4), obtained at several frequencies ($1Hz$, $50Hz$, $150Hz$ and $200Hz$) much below the first resonance frequency which is approximately $778Hz$ (from the identified model in Eq. (35)). As from the hysteresis curves, the actuator exhibits rate-dependent hysteresis behavior.

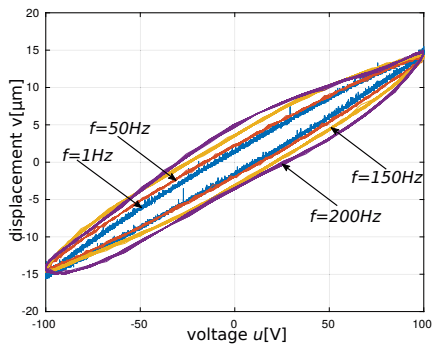

Fig. 4: Experimental hysteresis at different frequencies.

A rate-dependent Prandtl-Ishlinskii (RDPI) model $\hat{\Phi}[u(t)]$ was identified with the experimental data based on the four frequencies in Fig. (4). Then, an inverse RDPI model $u(t) = \hat{\Phi}^{-1}[v_r(t)]$ was derived and then put in cascade with the actuator as hysteresis compensator. Finally, the efficiency of the hysteresis compensator is tested with sine input signal $v_r(t)$ with frequencies from $1Hz$ to $200Hz$. Fig. (5) displays the results. They clearly show that, even for frequency that was not used for the identification, the compensation performance remains unchanged. The hysteresis is reduced from $\frac{8\mu m}{30\mu m} \approx 27\%$ (corresponding to $200Hz$ in Fig. (4)) to less than $\frac{1.5}{30} = 5\%$ (corresponding to $200Hz$ in Fig. (5)) while the average gain is unity ($v \approx v_r$).

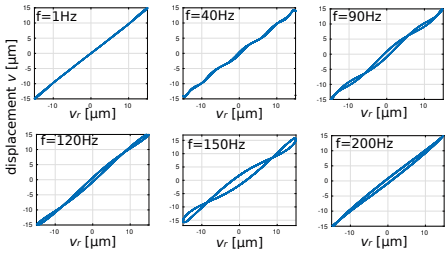

Fig. 5: Hysteresis compensation at different frequencies.

Then a step input $v_r = 15\mu m$ is applied to the actuator with hysteresis compensator. The normalized step response is shown in Fig. (6) (blue solid line) which reveals the badly damped oscillations property of the actuator. Such oscillations have to be attenuated or cancelled by the further interval RST controller.

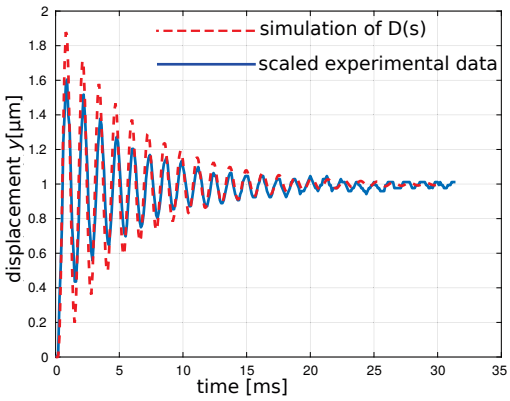

Fig. 6: Step response of the piezoelectric actuator with the RDPI inverse model.

C. The new model

The linear model $G(s) = kD(s)$ in Eq. (16) is identified in this section. First the static gain k is identified from Fig. (5). Since this gain is approximately 1, we suggest to bound it with the following interval, such that any future uncertainty (for e.g. due to temperature variation) be accounted for:

$$[k] = [0.8\mu m, 1.2\mu m] \tag{34}$$

Regarding the dynamics $D(s)$, its identification is made with the experimental step response in Fig. (6). The identified model is shown in Eq. (35) and its simulation is displayed in Fig. (6) (red dashed line) which indicates a good agreement with the experimental result.

$$D(s) = \frac{1}{41.83 \times 10^{-9}s^2 + 12.27 \times 10^{-6}s + 1} \tag{35}$$

In order to yield the interval model in Eq. (17), we consider each parameter of Eq. (35) as the center of the related interval parameter. The radius of each interval is taken as 20% of the center. The resulting interval parameters, listed in Eq. (36), are much larger than the intervals in [14], [16] where the radius are 10%. Thus, the uncertainty considered in this paper is wider and the RST controller is more robust.

$$\begin{cases} [a_2] = [37.647 \times 10^{-9}, 46.013 \times 10^{-9}] \\ [a_1] = [11.043 \times 10^{-6}, 13.497 \times 10^{-6}] \\ [k] = [0.8, 1.2] \end{cases} \tag{36}$$

D. Controller derivation and simulation of the closed-loop

The specification that is used to create the reference model in Eq. (27) and to calculate the controller parameters is: $t_{rmax} = 5ms$. This choice is because, additionally to the oscillations to be damped, we want to reduce the settling time which was initially $\approx 15ms$ (see Fig. (6)).

The controller parameters are calculated using the inclusions in Inclusion. (31) and the procedure in Section. (III-F). We obtain:

. $\mu_1 \in [0, 75.9 \times 10^{-9}]$. We select: $\mu_1 = 3.795 \times 10^{-9}$.

. $\mu_0 \in [-1.36 \times 10^{-6}, 0.41 \times 10{-}3]$. We select: $\mu_0 = 0.2 \times 10^{-3}$.

. $\rho_2 \in [0, 358 \times 10{-}9]$. We select: $\rho_2 = 179 \times 10^{-9}$.

. $\rho_1 \in [0, 2.15 \times 10{-}3]$. We select: $\rho_1 = 1.075 \times 10^{-3}$.

. $\rho_0 \in [0.833, 1.25]$. We select: $\rho_0 = 1.04$.

Finally, $T(s) = \rho_0 = 1.04$.

Note that we selected the middle of each interval solution for each controller parameter. However, any values taken in the intervals will satisfy the specifications as well.

The calculated RST controller is implemented and the closed-loop is simulated following the diagram in Fig. (3). For that, we apply the controller to the interval model $[G](s)$ with parameters in Eq. (36) and in Eq. (34). The response y to a step reference input $y_r = 15\mu m$ is displayed in Fig. (8-a) while the response y to a step disturbance $d = 1\mu m$ is displayed in Fig. (8-b). They clearly reveal the efficiency of the closed-loop to satisfy the desired behavior (without oscillations, simulated settling time $= 3.33ms$) and to reject the disturbance for any uncertainties within the interval model $[G](s)$.

E. Experimental results of the closed-loop

We now apply the RST controller to the real piezoelectric tube actuator with its hysteresis compensator, still following the diagram in Fig. (3). The result is shown in Fig. (8) which presents a step response without oscillations and with a settling time of $4ms$, and which demonstrate as well the efficiency of the proposed controller to satisfy the specifications.

V. Conclusion

A feedforward-feedback controller design for piezoelectric actuators with hysteresis and badly damped

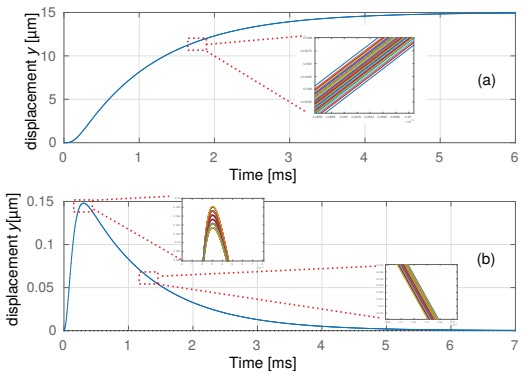

Fig. 7: Simulation of the closed-loop. (a): the response to a input reference step of $y_r = 15\mu m$ amplitude. (b): the response to a step disturbance of $d = 1\mu m$.

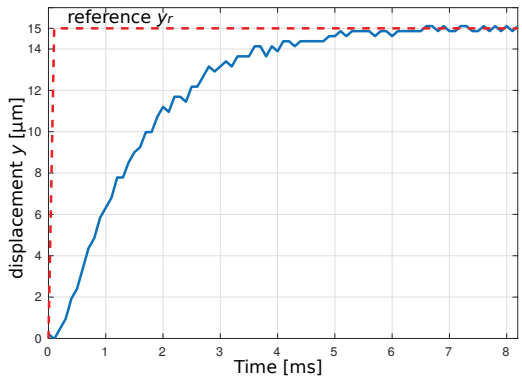

Fig. 8: Experimental result of the closed-loop: response to a input reference step of $y_r = 15\mu m$ amplitude.

oscillations was proposed in this paper. The feedforward controller was based on the rate-dependent Prandtl-Ishlinskii (RDPI) approach in order to reduce the rate-dependent hysteresis of the actuator. Then a RST controller structure was introduced for the feedback and a new interval design was proposed for that. The proposed controller design did not use set inversion problem, which eased the controller parameters calculation. Both simulation and experiments were carried out which demonstrated the efficiency of the proposed control design.

Acknowledgment

This work was supported by the national CODE-TRACK project (ANR-17-CE05-0014-01, Control theory tools for optimal design of piezoelectric energy harvesters devoted to birds tracking devices).

References

[1] J. L. Pons, "Emerging actuator technologies: a micromechatronic approach", Wiley, (ISBN 0-470-09197-5), 2005.

[2] M. Rakotondrabe, "Smart materials-based actuators at the micro/nano-scale: characterization, control and applications", Springer, New York, ISBN 978-1-4614-6683-3, 2013.

[3] G. Bining, C. F. Quate and Ch. Berger, "Atomic Force Microscope", Physical Review Letters, 56, pp.930-933, 1986.

[4] S. Devasia, E. E. Eleftheriou, R. Moheimani, "A survey of control issues in nanopositioning", IEEE TCST, Vol.15, pp.802-823, 2007.

[5] M. Rakotondrabe, "Bouc-Wen modeling and inverse multiplicative structure to compensate hysteresis nonlinearity in piezoelectric actuators", IEEE Trans ASE, April 2011.

[6] X. Tan and J. Baras, "Modeling and control of hysteresis in magnetostrictive actuators", Automatica, Vol.40, pp. 1469-1480, 2004.

[7] M. Al Janaideh and P. Krejci, "Inverse rate-dependent Prandtl-Ishlinskii model for feedforward compensation of hysteresis in a piezomicropositioning actuator", IEEE/ASME TMECH, vol.18, pp.1498-1507, 2013.

[8] M. Rakotondrabe, "Multivariable classical Prandtl-Ishlinskii hysteresis modeling and compensation and sensorless control of a nonlinear 2-dof piezoactuator," Nonlinear Dynamics, vol.89, pp.481-499, 2017.

[9] M. Al Janaideh and M. Rakotondrabe, "Control of Piezoelectric Positioning Systems using Inverse Rate-Dependent Prandtl-Ishlinskii Model and Performances Inclusion based Interval Techniques", Journal of Mathematical Modeling of Natural Phenomena, submitted, 2019.

[10] M. Kieffer, E. Walter, "Guaranteed estimation of the parameters of nonlinear continuous-time models: Contributions of interval analysis", International Journal of Adaptive Control and Signal Processing, Vol.25, p.191-207, 2011.

[11] B. Desrochers and L. Jaulin, "Computing a guaranteed approximation the zone explored by a robot", IEEE TAC, Vol.62, p.425-430, 2017.

[12] M. Rakotondrabe, "Performances inclusion for stable interval systems", American Control Conference, pp. 4367-4372, 2011.

[13] J. Bondia, M. Kieffer, E. Walter, J. Monreal and J. Picto, "Guaranteed tuning of PID controllers for parametric uncertain systems", CDC, 2948-2953, 2004.

[14] M. Hammouche, A. Mohand-Ousaid, P. Lutz, and M. Rakotondrabe, "Robust interval Luenberger observer-based state feedback control: application to a multi-DOF micropositioner", IEEE TCST, 2018.

[15] S. Khadraoui, M. Rakotondrabe, and P. Lutz, "Combining H-inf approach and interval tools to design a low order and robust controller for systems with parametric uncertainties: application to piezoelectric actuators", International Journal of Control, Vol.85, p.251-259, 2012.

[16] S. Khadraoui, M. Rakotondrabe and P. Lutz, "Interval Modeling and Robust Control of Piezoelectric Microactuators", IEEE TCST, Vol.20, pp. 486–494, 2012.

[17] S. Khadraoui, M. Rakotondrabe and P. Lutz, 'Design of RST-structured controller for parametric uncertain system using interval analysis: application to piezocantilever', Asian Journal of Control, Vol.15, 2013.

[18] M. Rakotondrabe, Y. Haddab and P. Lutz, "Quadrilateral modeling and robust control of a nonlinear piezoelectric cantilever", IEEE TCST, 17(3), pp.528-539, May 2009.

[19] H. Bourles, "Linear Systems", John Wiley Sons, ISBN 1848211627, 544pages, 2010.

[20] H. Xie, M. Rakotondrabe and S. Regnier, "Characterizing piezoscanner hysteresis and creep using optical levers and a reference nanopositioning stage", Review of Scientific Instruments, vol. 80, 046102, 2009.